

Fine structure in sunspots

II. Intensity variations and proper motions of umbral dots

Michal Sobotka¹, Peter N. Brandt², and George W. Simon³

¹ Astronomical Institute, Academy of Sciences of the Czech Republic, CZ-25165 Ondřejov, Czech Republic

² Kiepenheuer-Institut, D-79104 Freiburg, Germany

³ PL/GPSS, Sacramento Peak, Sunspot, NM 88349, USA

Received 25 March 1997 / Accepted 19 June 1997

Abstract. Temporal intensity variations of umbral dots (UDs) and dark nuclei (DNs), and proper motions of UD, were analyzed in a 4 1/2 hour time series of high resolution white light images of the umbra in a medium-size sunspot (NOAA 7519). The observations were made on 5 June 1993 at the Swedish Vacuum Solar Telescope, La Palma. An identification and tracking algorithm was applied to UD, observed in a destretched movie of 360 frames. In total, 662 UD, were tracked, and their intensities, positions, and proper motions were measured. Power spectra of temporal intensity variations of UD, and DN, were computed, and several typical periods were found. The histogram of time-averaged intensities of UD, has two maxima; the UD, belonging to the brighter part of the population are located mostly at or near the umbral-penumbral boundary. The number of UD, decreases with increasing magnitude of the proper motion velocity. Speeds of UD, are grouped at 100 and 400 m/s. The observed spatial distribution of UD, with different proper motion velocities is found to be in contradiction to the generally accepted idea of moving “peripheral” and stationary “central” UD, . Both “fast” and “slow” UD, are present in all parts of the umbra. Thus velocity does not appear to be a good criterion for separating UD, into “peripheral” and “central” ones.

Key words: Sun: sunspots – physical data and processes: convection

1. Introduction

Sunspot umbrae, observed at high spatial resolution, show a complex time-variable pattern of small-scale intensity fluctuations. The umbral brightenings are seen in the form of light bridges and umbral dots (UDs). The dark regions are formed by a diffuse background with an intensity that varies smoothly from one location to another. The darkest areas in the diffuse

background, which are almost void of UD, , are called dark nuclei (DN, , see Sobotka et al. 1993 for more details concerning the terminology used in this paper). UD, are sometimes divided into two classes (Grossmann-Doerth et al. 1986): “peripheral” UD, , located in the vicinity of the umbral-penumbral border, and “central” ones in the inner part of the umbra. “Peripheral” UD, are usually brighter than “central” ones.

UD, are dynamical objects. They appear, change their brightness, move, and disappear. Their lifetimes, as estimated by Beckers & Schröter (1968), Adjabshirzadeh & Koutchmy (1980), Kitai (1986), Kusoffsky & Lundstedt (1986), and Ewell (1992), range from several minutes to more than two hours. Adjabshirzadeh & Koutchmy (1980) attempted to measure temporal variations of radiative fluxes in 30 UD, . In 14 cases the variations had a unique character consisting of a rapid rise and a subsequent slow decrease of the flux.

An important attribute of UD, is their proper motion. It is known that bright penumbral grains flow inward toward the umbral-penumbral boundary (Muller 1973, Tönjes & Wöhl 1982). Similarly, many UD, , sometimes arising from or related to penumbral grains, move toward the umbral center with an average speed of about 400 m/s (Kitai 1986, Ewell 1992). Molowny-Horas (1994), using a more accurate method of velocity measurement, reported that the average speed of 28 UD, was 210 ± 50 m/s. Ewell (1992) observed that most of the moving UD, were located at the periphery of the umbra and suggested distinguishing between “central” and “peripheral” UD, on the basis of their proper motions – “central” UD, were stationary, while “peripheral” UD, drifted inwards. Sobotka et al. (1995) observed that proper motions of UD, were influenced by the spatial distribution of DN, . Most of the UD, slowed down and disappeared at the borders of DN, , or their trajectories were deflected. In several cases, a “collision” of a moving UD, with a DN, produced a brightening of another, already existing UD, , on the opposite side of the DN, . Kitai (1986) measured proper motions and lifetimes of “chromospheric UD, ”, bright features with sizes about $1''$, observed in H α filtergrams. He

found that “chromospheric UDs” with lifetimes larger than 10 minutes move with an average speed of 340 m/s.

In 1993, an 11 hour time series of high-resolution white-light images of solar granulation was obtained by Simon et al. (1994). During 4 1/2 hour a medium-size sunspot was also present in the field of view. Sobotka et al. (1997, hereafter Paper I) analyzed the temporal variations of the fine structure in the central umbral core of this spot and applied an identification and tracking algorithm to UDs present in its core. This enabled us to measure the lifetimes, observed sizes, filling factor, intensity variations, positions, and proper motions of a large sample of UDs. In Paper I we described our results on the filling factor, sizes, and lifetimes. We found that large (diameter $> 0''.4$) and long-lived (lifetime > 10 minutes) UDs appear mostly in regions with enhanced umbral diffuse background intensity. The measurements of the sizes and lifetimes have shown that UDs do not have a “typical” size. Their numbers increase rapidly with decreasing diameter down to the resolution limit. Similarly, UDs do not have a “typical” lifetime, and their numbers increase with decreasing lifetime. UDs with lifetimes shorter than 10 minutes represent about 2/3 of the population.

In Sect. 2 we will briefly summarize the observations, data reduction, and the UD identification and tracking procedures. We present our results on the temporal intensity variations of UDs and DNs, the corresponding power spectra, the spatial distribution of UDs with different intensities, and the proper motions of UDs in Sect. 3. Finally, in Sect. 4 we discuss the results.

2. Observations and data analysis

The observations, data reduction, the automatic identification and tracking algorithms, and the determination of image sharpness in the umbra are thoroughly described in Paper I. Therefore we give only a brief overview here:

The sunspot NOAA 7519 was observed at heliographic position N05, E15 on 5 June 1993 with the Swedish Vacuum Tower Telescope (SVST, aperture 50 cm) at La Palma, Canary Islands (Simon et al. 1994). A Kodak Megaplug Model 1.4 CCD camera was used to sample white light solar images at $\lambda 4680 \pm 50 \text{ \AA}$. The image scale was $0''.125/\text{pixel}$. Due to image rotation during the 11 hour time series, the sunspot was visible only for 4 hours 26 minutes, from 9:54 to 14:20 UT, during which we obtained 760 frames. These frames were registered, corrected for instrumental profile, and destretched, to minimize seeing distortions. From these we selected 360 with rms granulation contrast higher than 7%, covering almost regularly the whole time period. The selected frames were then interpolated in time to obtain a time series with a constant lag of 44.5 s.

For further analysis we selected a $8''.75 \times 8''.75$ (70×70 pixel) field covering the large central umbral core of the sunspot (cf. Fig. 1 of Paper I). UDs were isolated separately in each frame of the umbral core using an image segmentation method, based on an edge enhancement algorithm. An identification and tracking routine (cf. Paper I, Sect. 3) was then applied. From this procedure we obtained the lifetimes, intensities, effective

diameters, and positions of 662 UDs during their evolution. These UDs are the objects analyzed here and earlier in Paper I.

We used a different method to measure temporal intensity variations in DNs: Each DN was isolated in a $1'' \times 1''$ or $2'' \times 2''$ box, dependent on the size of the DN. We checked visually whether the DN remained in the box, and if the box was free of other DNs during the whole time series. If so, the intensity minimum in the box was recorded for each frame, so that the intensity of each DN was represented by the intensity of its darkest point.

For additional details of the analysis procedures and a discussion of stray light effects, the reader is referred to Paper I.

3. Results

3.1. Temporal intensity variations of umbral dots and dark nuclei

The identification and tracking algorithm yields directly the “light curve” for each UD. Examples of observed intensity variations (in units of the mean photospheric intensity I_{phot}) of 5 long-lived UDs are shown in Fig. 1: UD 26, located close to the center of the umbral core, was visible during the whole time series. It was “stationary”: the time-averaged velocity magnitude \bar{v} of the proper motion was 47 ± 1 m/s, i.e., it moved only about $1''$ in 266 minutes. UD 112 was the second-longest-lived UD. It appeared 32 minutes after the start of the series and lasted until the end. It was also stationary ($\bar{v} = 57 \pm 3$ m/s). UD 17 was also stationary ($\bar{v} = 52 \pm 6$ m/s). The abrupt increase in its intensity at 10:08 UT was preceded by partial penetration of a DN adjacent to UD 17 by a penumbral grain. During the penetration (at the side away from the UD) the speed and brightness of the penumbral grain continuously decreased until it disappeared. Finally, UDs 10 and 413 are examples of long-lived slowly moving UDs ($\bar{v} = 130 \pm 12$ and 168 ± 10 m/s, respectively). The time-averaged local background intensities corresponding to these 5 UDs are given by the intensities of nearby DNs. From top to bottom in Fig. 1 the values are: 0.20, 0.22, 0.22, 0.21, and 0.23.

In the previous paragraph we mentioned the brightening of UD 17 preceded by the “collision” of a penumbral grain with a DN located between the UD and the penumbra. Sobotka et al. (1995) reported that some UD brightenings may be related to collisions of penumbral grains or moving UDs with DNs lying between the colliding features and the brightened UDs. In the present time series we clearly identified 3 such brightenings with maxima at 10:08, 10:39, and 12:40 UT, which appeared 5, 9, and 6 minutes, respectively, after collisions of different penumbral grains and DNs located between the brightened UDs and the penumbra. The moment of the collision was defined as the moment of maximum deceleration of the penumbral grain. The distances between the UDs and the colliding penumbral grains were 1900, 1200, and 1800 km, respectively. If these brightenings were induced by some sort of perturbation propagating across the DNs, the velocities of propagation would range between 2 and 7 km/s.

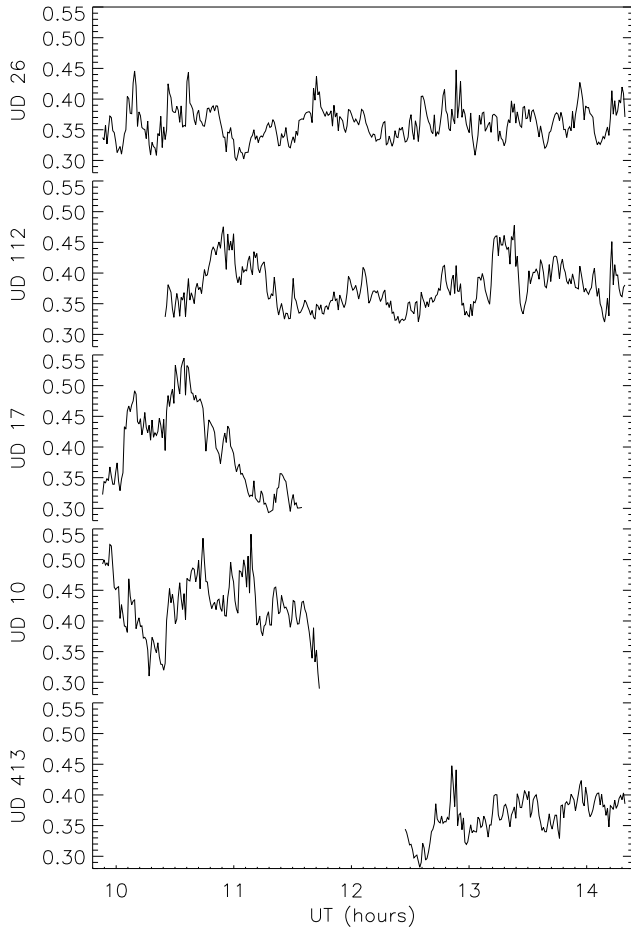


Fig. 1. Temporal intensity variations of 5 long-lived UDs. The observed intensities are in units of the mean photospheric intensity I_{phot} . The corresponding time-averaged local background intensities are (from top to bottom): 0.20, 0.22, 0.22, 0.21, and 0.23.

The umbral core under investigation contained 5 DNs. We obtained the temporal variations of observed minimum intensities for each DN. The lifetimes of DNs are much longer than those of UDs. Three were visible for the entire 4 hour 26 minute time series, and the other two for 4 hours 12 minutes and 3 hours 49 minutes. All the DNs showed temporal changes of their shape and in the location of the intensity minimum. In the darkest and largest DN the time-averaged observed intensity minimum was $(0.18 \pm 0.01) I_{\text{phot}}$, in which the standard deviation characterizes the magnitude of temporal variations.

With the aid of power spectra we analyzed the temporal intensity variations of these 5 DNs and of the 5 longest-lived UDs (lifetimes > 126 minutes). In order to reduce the noise, the individual power spectra of UDs (and similarly those of DNs) were averaged. To estimate possible false periods induced by seeing fluctuations, we also computed the power spectrum of image sharpness variations during the time series.

The result is shown in Fig. 2. For the DNs, arrows indicate peaks at periods of 14, 9.1, 3.4, 2.8, and 2.5 minutes. The 3.4 and 2.8 minute periods possibly reflect umbral oscillations, dis-

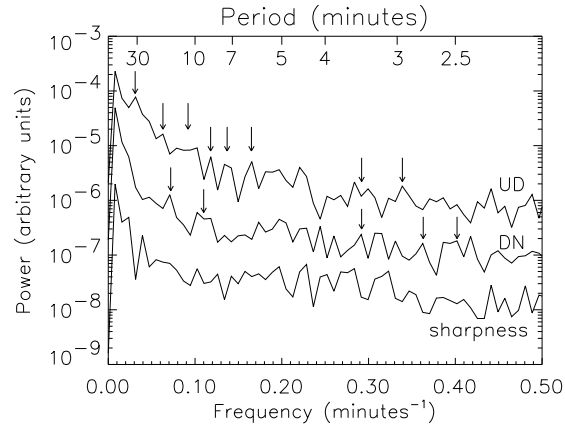


Fig. 2. Average power spectra of intensity variations of 5 long-lived umbral dots and of 5 dark nuclei, together with the power spectrum of image sharpness. Peaks mentioned in the text are marked by arrows.

torted by seeing and power spectrum noise. Umbral dots show enhancements of power at periods of 32, 16, 11, 8.5, 7.2, 6.1, 3.4 and 3.0 minutes. The peak at 32 minutes corresponds roughly to the average lifetime of UDs estimated by various authors (Adjabshirzadeh & Koutchmy 1980, Kitai 1986, Kusoffsky & Lundstedt 1986) and its harmonic at 16 minutes is also close to the lifetime reported by Ewell (1992). The 8.5 minute peak almost coincides with the broad 9.1 minute peak in DNs. The 3.4 minute and 3.0 minute periods could be interpreted as manifestation of umbral oscillations. Other periods, mostly in the vicinity of 4 and 5 minutes, coincide with peaks in the sharpness power spectrum and thus may be due to variations of the seeing rather than a real solar effect. Such “doubtful” peaks are not marked with arrows in Fig. 2. Although the peaks with arrows may not appear to be more significant than some of those without arrows, each of the peaks marked by an arrow was detected in all the individual power spectra of 5 UDs (and similarly in those of 5 DNs), while the peaks without arrows were not always present. Thus we conclude that those with arrows are significant while we are uncertain about the others. Note that the power corresponding to UDs is higher than that of DNs, because the intensity fluctuations in UDs are larger (at all frequencies) than in DNs.

Visual inspection of the “light curves” of several UDs with lifetimes between 30 and 90 minutes shows “bursts” of intensity with average duration of 30 minutes (similar bursts are also seen in long-lived UDs in Fig. 1, such as the 24 minute burst in UD 17 between 10:24 UT and 10:48 UT). This time interval corresponds well to the 32 minute period found in the power spectra of long-lived UDs.

3.2. Time-averaged brightness of umbral dots

To study the relation between the brightnesses and positions of UDs in the umbral core we calculated the time-averaged intensities of all 662 UDs in our sample. The histogram of time-averaged intensities is shown in Fig. 3. The two maxima at 0.34

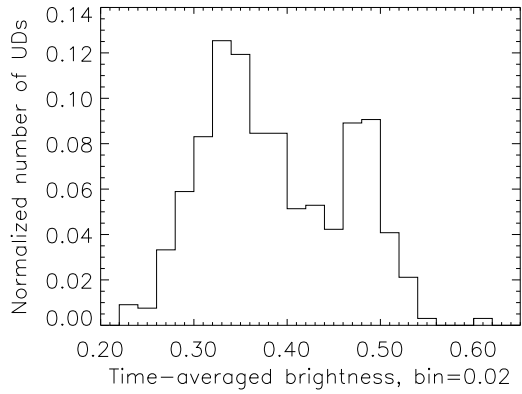


Fig. 3. Normalized number of UDs vs. time-averaged observed brightness (in units of I_{phot}) for 662 UDs.

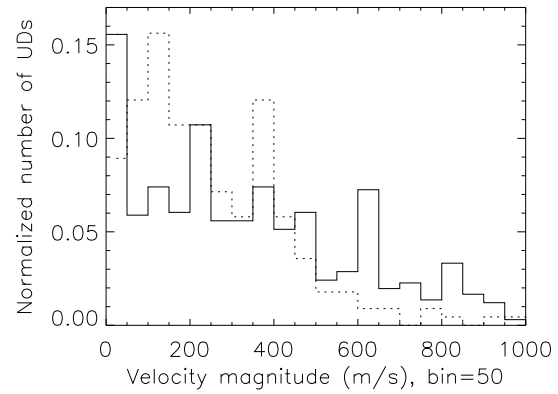


Fig. 5. Normalized number of UDs vs. magnitudes \bar{v} of time-averaged proper motion velocities \bar{v} for all 662 UDs (solid line) and for 224 UDs with lifetimes > 10 minutes (dashed line).

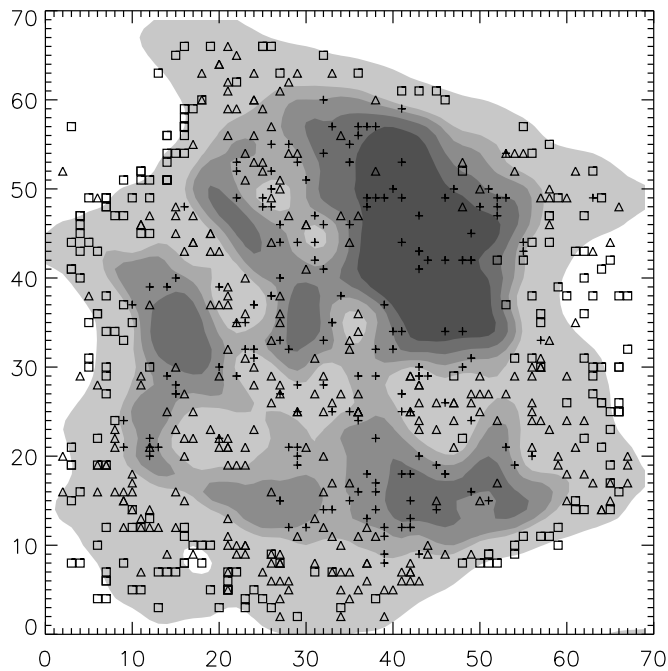


Fig. 4. Spatial distribution of 662 UDs with different time-averaged brightnesses \bar{I}_{ud} : Symbol “+” represents UDs with $\bar{I}_{\text{ud}} \leq 0.33$, triangles correspond to $0.33 < \bar{I}_{\text{ud}} \leq 0.43$, and squares to $\bar{I}_{\text{ud}} > 0.43 I_{\text{phot}}$. The underlying image of the umbral core is the average of 360 frames of the series with contours corresponding to intensities 0.24, 0.26, 0.28, 0.30, and $0.45 I_{\text{phot}}$. The coordinates are in pixels (scale $0''.125$ per pixel).

and $0.48 I_{\text{phot}}$ may indicate a double population of UDs, but we cannot say whether this is a general rule or an effect specific for this particular spot. The time-averaged positions of UDs with different average brightnesses are displayed in Fig. 4. The underlying contour image is the average of 360 frames of the series; it shows the positions of DNs and bright regions in the umbral core. We can see that UDs brighter than $0.43 I_{\text{phot}}$ (corresponding to the saddle in the histogram) are mostly located at or near the umbral-penumbral boundary, while fainter ones

occur everywhere in the umbra. DNs are either void of UDs or contain the weakest UDs.

Because the brightest (and thus best observable) UDs are concentrated near the umbral border, earlier observers suggested a division into “central” and “peripheral” UDs (Grossmann-Doerth et al. 1986). On the other hand, the enhanced brightness of UDs in the vicinity of the umbral border, where the intensity of the umbral diffuse background rises towards its maximum, is simply a consequence of the fact that the brightness of UDs is proportional to the intensity of the surrounding diffuse background (Sobotka et al. 1993). Some of the brightest objects at the umbral-penumbral boundary are actually not UDs but the bright “heads” of elongated penumbral grains or penumbral extensions.

We compared the time-averaged intensities with the lifetimes (derived in Paper I) of all 662 UDs in the sample and found no correlation between them.

3.3. Proper motions of umbral dots

We characterize the proper motions of UDs by vectors of time-averaged velocities \bar{v} . First consider the magnitudes \bar{v} . The measurement accuracy, using least-squares linear fits to the positions of UDs (cf. Molowny-Horas 1994), obviously increases with increasing lifetime — the standard deviations of \bar{v} are approximately 200 m/s for UDs with lifetimes < 10 minutes, but 35 m/s for lifetimes > 10 minutes and 20 m/s for lifetimes > 20 minutes.

The normalized histograms are plotted in Fig. 5, in which the solid line represents all 662 UDs in the sample, and the dashed one corresponds to the 224 UDs with lifetimes longer than 10 minutes. The general trend is that the number of UDs decreases with increasing \bar{v} . The histogram of the total sample has local maxima at 0 (absolute maximum), 200, and 600 m/s. UDs with lifetimes > 10 minutes, for which the measurements of \bar{v} are more accurate, show maxima at 100 (absolute maximum) and 400 m/s. The maxima have the form of isolated peaks which protrude from a monotonically decreasing distribution. If

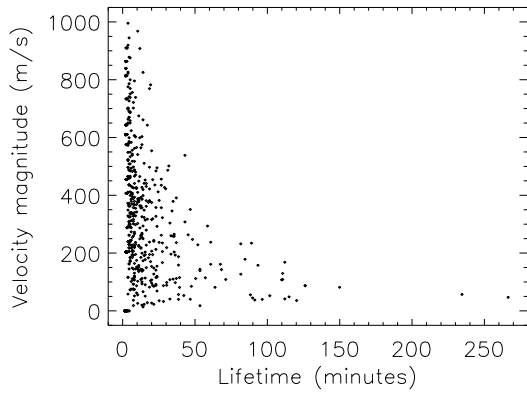


Fig. 6. Scatter diagram of time-averaged proper motion velocity magnitude \bar{v} vs. lifetime of 662 UDs.

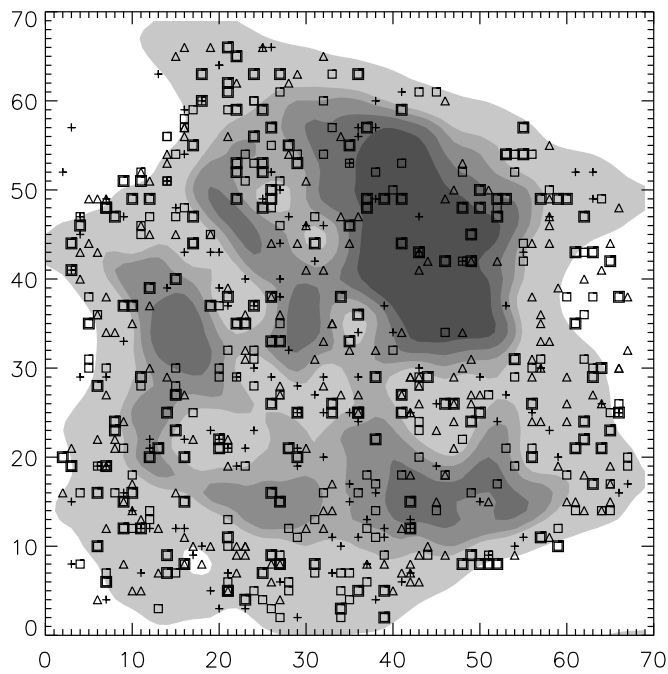


Fig. 7. Spatial distribution of 662 UDs with different \bar{v} : Symbol “+” represents UDs with $\bar{v} \leq 100$ m/s, triangles correspond to $100 < \bar{v} \leq 300$ m/s, squares to $300 < \bar{v} \leq 500$ m/s, and bold squares to $\bar{v} > 500$ m/s. The underlying grey-scale image and scale are as in Fig. 4.

we fit least-squares second-order polynomials to both distributions and compute the deviations of the data from the fits, then we note that the maxima appear to be statistical fluctuations in the case of the total sample (Fig. 5, full line), but are significant at the level of 2σ in the case of the UDs that live longer than 10 minutes. From this we conclude that, in the latter case, these peaks represent different populations of UD velocities.

A scatter diagram of \bar{v} versus lifetime (similar to that for “chromospheric UDs” presented by Kitai 1986, Fig. 10) is shown in Fig. 6. We can see that the maximum \bar{v} decreases with lifetime.

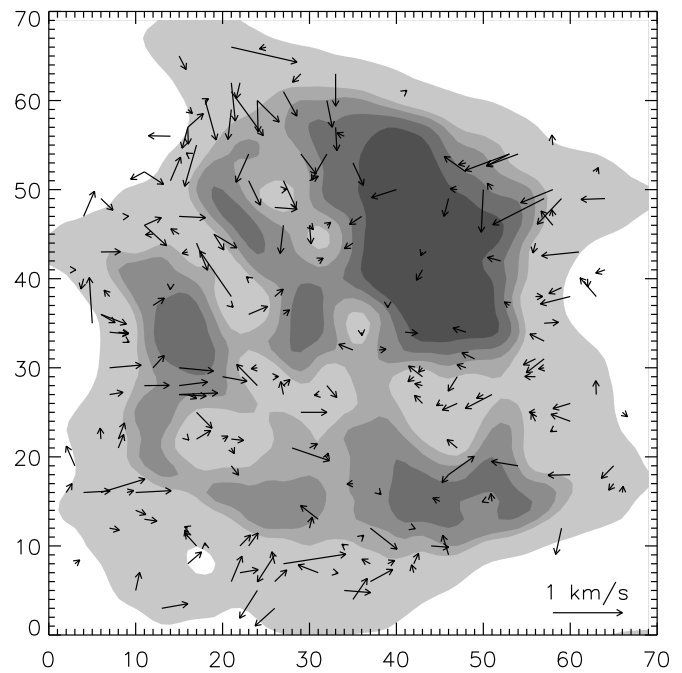


Fig. 8. Vectors of time-averaged proper motion velocities for 224 UDs with lifetimes > 10 minutes. Origins of vectors are located at time-averaged positions of UDs. The underlying grey-scale image and scale are as in Fig. 4.

The spatial distribution of 662 UDs with different \bar{v} is displayed in Fig. 7. According to Ewell (1992), who distinguished between “central” and “peripheral” UDs on the basis of their proper motions, we would expect a substantial concentration of rapidly moving “peripheral” UDs near the umbral border. This effect, however, is not observed in Fig. 7. Both “fast” and “slow” UDs are present in all parts of the umbra. Although the concentration of the brightest UDs near the umbral-penumbral boundary (see Sect. 3.2) might give reason to call them “peripheral” UDs, only 43% of them are moving faster than 300 m/s and 20% faster than 500 m/s.

When we restrict our sample to the 224 UDs with lifetimes longer than 10 minutes, the velocities seem slightly more organized. In Fig. 8 we plot the time-averaged velocity vectors for these UDs. We can see the inward direction of UD proper motions at the periphery and slowly moving UDs in the central part of the umbra. When we calculate the mean \bar{v} of 44 UDs located within $1''$ of the geometrical center of the umbra and compare it with the mean \bar{v} of 180 UDs at distances $> 1''$ from the center, we obtain 180 and 270 m/s, respectively. Nevertheless, moving and stationary UDs can be found at any location in the umbra. These data *do not support the claims of other authors that UDs can be divided into “central” and “peripheral” on the basis of their proper motions.*

4. Discussion and conclusions

From a 4 1/2 hour time series of excellent quality, we analyzed a sample of 662 UD, obtained by an object-tracking procedure. In Paper I we described results concerning the filling factor, sizes, and lifetimes of UD. The main results of the present paper can be summarized as follows:

1. We confirm the previous observations of Sobotka et al. (1995) who reported that the “collisions” of penumbral grains or moving UD with DN (during which the moving features decelerate, weaken, and finally disappear) are sometimes followed by brightenings of already existing UD on the opposite side of the DN. In the present data we identified 3 such brightenings. If the collision and subsequent brightening are physically related, e.g. by a wave propagating across the DN, the propagation speed would be about 2 – 7 km/s. This effect needs further observational confirmation and a physical interpretation.

2. The power-spectra analysis of temporal intensity variations of long-lived UD revealed, in addition to 3-minute umbral oscillations, also periods of 32, 16, 11, 8.5, 7.2, and 6.1 minutes. We suggest that the earlier estimates of “typical” lifetimes of UD (26, 40, and 15 minutes) reported by Adjabshirzadeh & Koutchmy (1980), Kitai (1986), and Ewell (1992), respectively, may have been affected by the 32 and 16 minute periods of the UD intensity variations that we have found from our data. In Fig. 5 of Paper I we showed that UD do not have any “typical” lifetime; rather, the shorter the lifetime, the more numerous they are.

3. The histogram of time-averaged intensities of UD (Fig. 3) shows two clearly separated maxima. Since there are no similar data sets for other sunspots, we cannot conclude whether this is an accidental effect or it is the usual case. UD belonging to the brighter population in the histogram are located mostly at, or near, the umbral-penumbral boundary. This probably led earlier observers to the division into “central” and “peripheral” UD. Since the intensity of the diffuse background rises to its maximum at the periphery of the umbra, the presence of the brightest UD in this region confirms the relation of proportionality between the brightness of UD and the adjacent diffuse background as found by Sobotka et al. (1993).

4. The number of UD decreases with increasing magnitude of the proper motion velocity. Isolated peaks at 100 and 400 m/s (for UD with lifetimes > 10 minutes) are superposed on this nearly monotonic distribution. This result is consistent with earlier measurements by Kitai (1986) and Molowny-Horas (1994) made for small samples of UD.

5. The observed spatial distribution of UD with different proper motion velocities is in contradiction to the generally accepted idea of moving “peripheral” and stationary “central” UD. Both “fast” and “slow” UD are present in all parts of the umbra. This is a somewhat surprising result, obtained by our identification and tracking algorithm applied to a large sample of UD. Why did earlier observers (Kitai 1986, Ewell 1992, Molowny-Horas 1994, Sobotka et al. 1995) see moving “peripheral” and stationary “central” UD in their movies? The human eye appears to be attracted by UD with relatively longer

lifetimes, which can be followed more easily. If we restrict our sample to UD with lifetimes longer than 10 minutes, the velocities of UD at the periphery of the umbra are indeed higher in average than those in the central part, and the prevailing inward direction of motions at the periphery can be detected. Although moving UD with lifetimes > 10 minutes appear more frequently in the outer regions of the umbra, in general moving and stationary UD can be found at the periphery as well as in the central part. Thus velocity does not appear to be a good criterion for separating UD into “peripheral” and “central” ones.

Acknowledgements. We acknowledge the efficient support by M. Barreto, G. Hosinsky, R. Kever, G. Scharmer, and W. Wang during the observations at La Palma. Technical and financial support was provided by Mark Shand of DEC’s Paris office. M.S. gratefully acknowledges grants by the Deutsche Forschungsgemeinschaft (436 TSE 17/5/95) and by the Grant Agency of the Academy of Sciences of the Czech Republic (A 3003601). This work was accomplished under the Key Project K1-003-601 of the Academy of Sciences of the Czech Republic. The Swedish Vacuum Tower Telescope is operated by the Swedish Royal Academy of Sciences at the Spanish Observatorio del Roque de los Muchachos of the Instituto de Astrofísica de Canarias. Both the Air Force Office of Scientific Research and the Kiepenheuer-Institut für Sonnenphysik provided support to G.W.S. for this project, while P.N.B. received travel funds from AFOSR’s European Office for Aerospace Research.

References

- Adjabshirzadeh A., Koutchmy S., 1980, *A&A* 89, 88
 Beckers J. M., Schröter E. H., 1968, *Solar Phys.* 4, 303
 Ewell M. W., 1992, *Solar Phys.* 137, 215
 Grossmann-Doerth U., Schmidt W., Schröter E. H., 1986, *A&A* 156, 347
 Kitai R., 1986, *Solar Phys.* 104, 287
 Kusoffsky U., Lundstedt H., 1986, *A&A* 160, 51
 Molowny-Horas R., 1994, *Solar Phys.* 154, 29
 Muller R., 1973, *Solar Phys.* 29, 55
 Simon G. W., Brandt P. N., November L. J., Scharmer G. B., Shine R. A., 1994, in: *Solar Surface Magnetism*, eds. R. J. Rutten, C. J. Schrijver, Kluwer, Dordrecht, p. 261
 Sobotka M., Bonet J. A., Vázquez M., 1993, *ApJ* 415, 832
 Sobotka M., Bonet J. A., Vázquez M., Hanslmeier A., 1995, *ApJ* 447, L133
 Sobotka M., Brandt P. N., Simon G. W., 1997, *A&A* 328, 682
 Tönjes K., Wöhl H., 1982, *Solar Phys.* 75, 63